Available online at www.sciencedirect.com
ScienceDirect
Journal of Sound and Vibration 302 (2007) 313–331
JOURNAL OF SOUND AND VIBRATION
www.elsevier.com/locate/jsvi

# Rayleigh–Lamb waves in a microstretch elastic plate cladded with liquid layers

Dilbag Singh, S.K. Tomar*

*Department of Mathematics, Panjab University, Chandigarh 160 014, India*

Received 26 April 2006; received in revised form 28 September 2006; accepted 3 December 2006
Available online 16 January 2007

**Abstract**

Propagation of Rayleigh–Lamb waves in an infinite plate of finite thickness and composed of microstretch elastic material is considered. The top and bottom of the plate are cladded with finite layers of a homogeneous and inviscid liquid (non-micropolar and non-microstretch). There exist two sets of boundary conditions at solid/liquid interface and the choice on these sets of boundary conditions is arbitrary. Frequency equations are derived for symmetric and antisymmetric modes of propagation for Rayleigh–Lamb waves propagation. It is found that the frequency equations for both the modes of propagation are dispersive in nature and the presence of microstretch has negligible effect on the dispersion curves. However, the attenuation coefficient is found to be influenced by the presence of microstretch in the plate with free boundaries. Considerable effect of the liquid layers is noticed on the dispersion curves. Numerical computations are performed for a specific model to compute the phase velocity and attenuation coefficient for different values of wavenumber, for both symmetric and antisymmetric vibrations. Results of some earlier workers have been deduced as special cases.


## 1. Introduction

The problem of wave propagation in an elastic plate of uniform material was first investigated by Lamb [1]. Since then the term 'Lamb wave' has been used to refer to an elastic disturbance propagating in a solid plate with free boundaries. Lamb waves have found applications in multi-sensors and in the inspection of defects in thin-walled materials. The density and viscosity sensing with Lamb waves is based on the principle that the presence of liquid in contact with a solid plate changes the velocity and amplitude of the Lamb waves in the plate with free boundaries. When a plate of finite thickness is bordered with homogeneous liquid half-spaces on both sides then some part of the Lamb wave energy in the plate radiates into the liquid, while most of the energy still remains in the solid. These are known as leaky Lamb waves. Wu and Zhu [2] and Zhu and Wu [3] studied the propagation of Lamb waves in an elastic plate when both sides of the plate are bordered with liquid layers. Sharma et al. [4] have also studied thermoelastic Lamb waves in a transversely isotropic plate bordered with layers of inviscid liquid. Sharma and Pathania [5] studied the thermoelastic waves in a plate

*Corresponding author.
*E-mail addresses:* kahlondilbag@yahoo.com (D. Singh), sktomar@yahoo.com (S.K. Tomar).

0022-460X/$ - see front matter © 2006 Elsevier Ltd. All rights reserved.
doi:10.1016/j.jsv.2006.12.002

bordered with inviscid liquid layers. They obtained the dispersion equations of Lamb waves and investigated them in details. Literature dealing with the wave propagation in elastic plate of finite thickness and of infinite extent may be found in several books, e.g. Ewing et al. [6], Viktorov [7], Graff [8]. The papers by Chimenti [9], Shuvalov [10], Rogers [11] including many others are notable in this pertinent area of research.

Eringen and his co-worker [12,13] developed a nonlinear theory of simple microelastic solids. Later, Eringen [14,15] developed a linear theory of micropolar elasticity which is a subclass of the theory of micromorphic material earlier developed by him [16]. In classical theory of elasticity, the points of the material have translational degrees of freedom and the transmission of the load across a differential element of the surface is described by a force vector only. However, in the theory of micropolar elasticity, there is an additional degree of freedom characterized by rotation of material points, and there is an additional kind of stress called couple stress. Thus, in the classical theory of elasticity, the effect of couple stress is neglected. Later, Eringen [17] developed a linear theory of thermo-microstretch elastic solid, which is a generalization of the linear theory of micropolar elasticity and is again a subclass of the theory of micromorphic materials [16]. In microstretch elastic solids, the material particles can undergo translation, rotation and stretches (contraction or extension). The motion in microstretch elastic solids is characterized by seven degrees of freedom comprising 3-translation, 3-rotation and 1-stretch. The transmission of load across a differential element of the surface of a microstretch elastic solid is described by a force vector, a couple stress vector and a microstretch vector. The theory of microstretch elastic solid differs from the theory of micropolar elasticity in the sense that there is an additional degree of freedom called stretch and there is an additional kind of stress called microstretch vector. The materials like porous elastic material filled with gas or inviscid fluid, asphalt, composite fibers, etc. lie in the category of microstretch elastic solids. The references in Refs. [12,13,18] have extensive literature on the present field of research. Frequency equations for Lamb wave propagation in a micropolar plate bordered with inviscid liquid layers was obtained by Tomar [19]. Recently, Tomar [20] investigated the propagation of Rayleigh–Lamb waves in a plate of micropolar elastic material with voids.

In practical situations, it is extremely important to detect hidden cracks (and other possible faults) in aerospace and other structures. This can be done by using ultrasonic waves. Lamb waves (which direct the energy along the plate) are especially useful in thin plates. The other applications are in radar detection. Recently, resurgent interest in Lamb waves is initiated by its applications in multisensors.

In the present work, we have discussed the propagation of Rayleigh–Lamb waves in a plate of homogeneous and isotropic microstretch elastic material cladded with layers of same liquid. The liquid is assumed to be homogeneous, inviscid and non-polar. The field equations and constitutive relations for microstretch elastic material developed by Eringen are employed for mathematical analysis. The frequency equations corresponding to symmetric and antisymmetric modes of vibrations of the plate are obtained. These frequency equations are discussed for some limiting cases and some known results of earlier authors have been reduced. Phase velocity and attenuation coefficient are also computed for a specific model and the effect of microstretch is noticed on them.

## 2. Problem and basic equations

We consider a plate of finite thickness '$2d$' and composed of a microstretch elastic solid material. The plate is assumed to be of infinite extent in the $x-y$ plane, whose top and bottom faces are bordered with layers of a homogeneous inviscid liquid of thickness '$h$'. The $x-y$ plane is taken to coincide with the middle plane of the plate and the $z$-axis is taken normal to it along the thickness of the plate. The complete geometry of the problem is shown in Fig. 1. We shall discuss the propagation of Rayleigh–Lamb waves in a two-dimensional $x-z$ plane.

The equations of motion in a linear homogeneous and isotropic microstretch elastic solid medium, in the absence of body force, body couple and microstretch body force, are given by [18, pp. 254–255]

$$(c_1^2+c_3^2)\nabla(\nabla\cdot\mathbf{U})-(c_2^2+c_3^2)\nabla\times(\nabla\times\mathbf{U})+c_3^2\nabla\times\mathbf{L}+\bar{\lambda_0}\nabla\Pi=\ddot{\mathbf{U}}, \tag{1}$$

$$(c_4^2+c_5^2)\nabla(\nabla\cdot\mathbf{L})-c_4^2\nabla\times(\nabla\times\mathbf{L})+\omega_0^2\nabla\times\mathbf{U}-2\omega_0^2\mathbf{L}=\ddot{\mathbf{L}}, \tag{2}$$

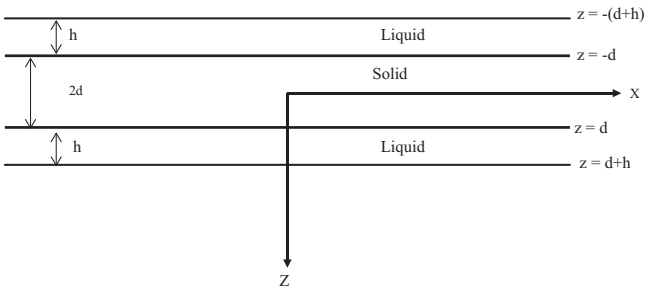


Fig. 1. Geometry of the problem.

$$c_6^2\nabla^2\Pi - c_7^2\Pi - c_8^2\nabla\cdot\mathbf{U} = \ddot{\Pi}, \tag{3}$$

where $c_1^2 = (\lambda+2\mu)/\rho$, $c_2^2 = \mu/\rho$, $c_3^2 = K/\rho$, $c_4^2 = \gamma/\rho j$, $c_5^2 = (\alpha+\beta)/\rho j$, $\omega_0^2 = c_3^2/j$, $c_6^2 = 2\alpha_0/\rho j$, $c_7^2 = 2\lambda_1/3\rho j$, $c_8^2 = 2\lambda_0/3\rho j$, $\bar{\lambda}_0 = \lambda_0/\rho$; $\lambda$ and $\mu$ are Lame's parameters, $K$, $\alpha$, $\beta$ and $\gamma$ are micropolar constants, $\lambda_0$, $\lambda_1$ and $\alpha_0$ are microstretch constants, $\rho$ is the density of the medium, $j$ is the micro-inertia, $\mathbf{U}$ and $\mathbf{L}$ are the displacement and microrotation vectors, respectively, and $\Pi$ is the scalar microstretch. Superposed dots on right-hand sides of Eqs. (1)–(3) indicate the temporal derivatives and other symbols have their usual meanings.

The constitutive relations in a linear homogeneous and isotropic microstretch elastic solid medium are given by [18]

$$\tau_{kl} = \lambda U_{r,r}\delta_{kl} + \mu(U_{k,l} + U_{l,k}) + K(U_{l,k} - \varepsilon_{klr}L_r) + \lambda_0\Pi\delta_{kl}, \tag{4}$$

$$m_{kl} = \alpha L_{r,r}\delta_{kl} + \beta L_{k,l} + \gamma L_{l,k}, \tag{5}$$

$$\beta_k = \alpha_0\Pi_{,k}, \tag{6}$$

where $\tau_{kl}$ is the force stress tensor, $m_{kl}$ is the couple stress tensor and $\beta_k$ is the microstretch tensor. Other symbols have their usual meanings.

Since we are discussing a two-dimensional problem in $x-z$ plane, so we shall take the following components of displacement vector, microrotation vector and scalar microstretch, respectively, as

$$\mathbf{U} = (u(x,z), 0, w(x,z)), \quad \mathbf{L} = (0, L(x,z), 0), \quad \Pi = \Pi(x,z).$$

With these considerations and using potentials $\phi$ and $\psi$ such that

$$u = \frac{\partial\phi}{\partial x} + \frac{\partial\psi}{\partial z}, \quad w = \frac{\partial\phi}{\partial z} - \frac{\partial\psi}{\partial x},$$

into Eqs. (1)–(3), we obtain

$$(\lambda+2\mu+K)\nabla^2\phi + \lambda_0\Pi = \rho\frac{\partial^2\phi}{\partial t^2}, \tag{7}$$

$$(\mu+K)\nabla^2\psi - KL = \rho\frac{\partial^2\psi}{\partial t^2}, \tag{8}$$

$$\gamma\nabla^2 L + K\nabla^2\psi - 2KL = \rho j\frac{\partial^2 L}{\partial t^2}, \tag{9}$$

$$6\alpha_0\nabla^2\Pi - 2\lambda_0\nabla^2\phi - 2\lambda_1\Pi = 3\rho j\frac{\partial^2\Pi}{\partial t^2}. \tag{10}$$

It can be seen that Eqs. (7) and (10) are coupled in $\phi$ and $\Pi$, while Eqs. (8) and (9) are coupled in $\psi$ and $L$. To find out the time harmonic solution of these equations, we assume the form of $\psi$, $\phi$, $L$ and $\Pi$ as follows:

$$\{\phi,\psi,L,\Pi\}(x,z,t) = \{\bar{\phi},\bar{\psi},\bar{L},\bar{\Pi}\}(x,z)\exp\{-\mathrm{i}\omega t\}, \tag{11}$$

where $\omega$ is an angular frequency, which is related to the wavenumber $\xi$ and phase velocity $c$ through the relation $\omega = \xi c$. Substituting Eq. (11) into Eqs. (7)–(10), we obtain

$$(\lambda + 2\mu + K)\nabla^2\bar{\phi} + \lambda_0\bar{\Pi} = -\rho\omega^2\bar{\phi}, \tag{12}$$

$$(\mu + K)\nabla^2\bar{\psi} - K\bar{L} = -\rho\omega^2\bar{\psi}, \tag{13}$$

$$\gamma\nabla^2\bar{L} + K\nabla^2\bar{\psi} - 2K\bar{L} = -\rho j\omega^2\bar{L}, \tag{14}$$

$$6\alpha_0\nabla^2\bar{\Pi} - 2\lambda_0\nabla^2\bar{\phi} - 2\lambda_1\bar{\Pi} = -3\rho j\omega^2\bar{\Pi}. \tag{15}$$

Again, we can see that Eqs. (12) and (15) are coupled in potentials $\bar{\phi}$ and $\bar{\Pi}$, while Eqs. (13) and (14) are coupled in potentials $\bar{\psi}$ and $\bar{L}$. By elimination procedure, it can be seen that these potentials satisfy the following:

$$[\nabla^4 + \ell_1\nabla^2 + \ell_2](\bar{\Pi}, \bar{\phi}) = 0, \tag{16}$$

$$[\nabla^4 + \ell_3\nabla^2 + \ell_4](\bar{L}, \bar{\psi}) = 0, \tag{17}$$

where

$$\ell_1 = \left(\frac{3\rho j\omega^2 - 2\lambda_1}{6\alpha_0} + \frac{3\alpha_0\rho\omega^2 + \lambda_0^2}{3\alpha_0(\lambda + 2\mu + K)}\right), \quad \ell_2 = \frac{\rho\omega^2(3\rho j\omega^2 - 2\lambda_1)}{6\alpha_0(\lambda + 2\mu + K)},$$

$$\ell_3 = \left(\frac{\rho j\omega^2 - 2K}{\gamma} + \frac{\gamma\rho\omega^2 + K^2}{\gamma(\mu + K)}\right), \quad \ell_4 = \frac{\rho K\omega^2}{\gamma(\mu + K)}\left(\frac{\rho j\omega^2}{K} - 2\right).$$

The solutions of Eqs. (16) and (17) can be obtained easily and finally the time harmonic solutions of Eqs. (7)–(10) can be written as

$$\phi = (A\sinh Rz + B\cosh Rz + C\sinh Sz + D\cosh Sz)\mathrm{e}^{\mathrm{i}(\xi x - \omega t)}, \tag{18}$$

$$\Pi = a(A\sinh Rz + B\cosh Rz) + b(C\sinh Sz + D\cosh Sz)\mathrm{e}^{\mathrm{i}(\xi x - \omega t)}, \tag{19}$$

$$\psi = (E\sinh Pz + F\cosh Pz + G\sinh Qz + H\cosh Qz)\mathrm{e}^{\mathrm{i}(\xi x - \omega t)}, \tag{20}$$

$$L = c'(E\sinh Pz + F\cosh Pz) + d'(G\sinh Qz + H\cosh Qz)\mathrm{e}^{\mathrm{i}(\xi x - \omega t)}, \tag{21}$$

where the coupling constants $a$, $b$, $c'$ and $d'$ are given by

$$a = -\{(c_1^2 + c_3^2)(-\xi^2 + R^2) + \omega^2\}/\bar{\lambda}_0, \quad b = -\{(c_1^2 + c_3^2)(-\xi^2 + S^2) + \omega^2\}/\bar{\lambda}_0,$$

$$c' = \{(c_2^2 + c_3^2)(-\xi^2 + P^2) + \omega^2\}/c_3^2, \quad d' = \{(c_2^2 + c_3^2)(-\xi^2 + Q^2) + \omega^2\}/c_3^2$$

and the expressions of $R$, $S$, $P$ and $Q$ are given by

$$R^2, S^2 = \xi^2 - \tfrac{1}{2}[\ell_1 \pm \sqrt{\ell_1^2 - 4\ell_2}], \quad P^2, Q^2 = \xi^2 - \tfrac{1}{2}[\ell_3 \pm \sqrt{\ell_3^2 - 4\ell_4}].$$

The expressions of $R^2$ and $P^2$ are taken with '+' sign and the expressions of $S^2$ and $Q^2$ are taken with '−' sign.

The equation of motion in liquid medium is given by

$$\nabla^2 \Psi = \frac{1}{c_L^2} \frac{\partial^2 \Psi}{\partial t^2}, \tag{22}$$

where $\Psi$ is the displacement potential and $c_L = \sqrt{\lambda_L/\rho_L}$ is the velocity of sound in liquid, $\lambda_L$ and $\rho_L$ being the bulk modulus and density of the liquid, respectively.

Denoting the displacement potential function by $\phi_{L_1}$ and $\phi_{L_2}$ for the top and bottom layers of the liquid, respectively, the normal component of displacement $w_{L_i}$ and pressure $p$ in the liquid medium are given by

$$w_{L_i} = \frac{\partial \phi_{L_i}}{\partial z}, \quad p = \rho_L \omega^2 \phi_{L_i} \tag{23}$$

($i = 1$ for the liquid in top layer and $i = 2$ for the liquid in bottom layer).

The time harmonic solutions of Eq. (22) in top and bottom liquid layers are given by (see Ref. [2])

$$\phi_{L_1} = F_1 \sin\{T[z - (d+h)]\} e^{i(\xi x - \omega t)} \quad \text{for } [d \leqslant z \leqslant (d+h)], \tag{24}$$

$$\phi_{L_2} = F_2 \sin\{T[z + (d+h)]\} e^{i(\xi x - \omega t)} \quad \text{for } [-(d+h) \leqslant z \leqslant -d], \tag{25}$$

where $F_1$ and $F_2$ are unknown, $T^2 = K_L^2 - \xi^2$ and $K_L = \omega/c_L$.

To derive the frequency equation for Rayleigh–Lamb waves in the plate considered, we shall use the following boundary conditions at the solid–liquid interfaces.

## 3. Boundary conditions

Since we are considering an inviscid liquid, the relevant boundary conditions at the solid/liquid interface will be the continuity of displacement and stresses. Since the liquid does not support shear stress, therefore, at liquid–solid interface, the normal stress must be equal to the pressure in the liquid layer and shear stress must vanish. Also, as one cannot protect the flow of liquid over a solid, the continuity condition cannot be put on displacement component along $x$-axis, however normal component of displacement must be continuous at liquid–solid interface. Mathematically, these boundary conditions are

$$\tau_{zx} = 0, \quad \tau_{zz} = -p \quad \text{and} \quad w = w_L. \tag{26}$$

These constitute three boundary conditions. However, to solve a boundary-value problem at the interface of interest, we need two more conditions. The balance of moment of momentum across the interface of two microstretch elastic solids requires the continuity of normal component of couple stress and continuity of microstretch vector. In the present instance, we have the interface between a microstretch elastic solid and an inviscid liquid. Since our liquid neither exhibit micropolarity nor microstretch property, therefore, at liquid–solid interface, the couple stress tensor and the microstretch tensor must vanish. These conditions can be written as

$$m_{zy} = 0 \quad \text{and} \quad \beta_z = 0. \tag{27}$$

These are the remaining two boundary conditions we need.

The boundary conditions on the displacement fields are purely kinematic, so the boundary conditions on microrotation and microstretch cannot be ruled out. We see that other set of boundary conditions are also possible for the present case. These are the vanishing of microrotation and microstretch of the solid at liquid–solid interface as our liquid cannot support both (however, one can consider such a liquid in which both microrotation and microstretch are non-null). Therefore, one can use the following boundary conditions in place of those given in Eq. (27):

$$L = 0 \quad \text{and} \quad \Pi = 0. \tag{28}$$

Thus, we see that there are two sets of boundary conditions at the solid–liquid interfaces $z = \pm d$. These are:

**Set I:** $\tau_{zx} = 0$, $m_{zy} = 0$, $\beta_z = 0$, $\tau_{zz} = -p$, $w = w_L$.

**Set II:** $\tau_{zx} = 0$, $L = 0$, $\Pi = 0$, $\tau_{zz} = -p$, $w = w_L$.

Using Eqs. (18)–(21), (23)–(25) and relevant quantities from Eqs. (4)–(6) into the boundary conditions given in Set-I, we shall obtain the following 10 homogeneous equations in 10 unknown, namely $A$, $B$, $C$, $D$, $E$, $F$, $G$, $H$, $F_1$ and $F_2$, given by

$$[-\lambda\xi^2+(\lambda+2\mu+K)R^2+\lambda_0 a](A\sinh Rd+B\cosh Rd)+[-\lambda\xi^2+(\lambda+2\mu+K)S^2+\lambda_0 b]\times(C\sinh Sd+D\cosh Sd)-\mathrm{i}\xi P(2\mu+K)(E\cosh Pd+F\sinh Pd)-\mathrm{i}\xi Q(2\mu+K)\times(G\cosh Qd+H\sinh Qd)-\rho_L\omega^2F_1\sin Th=0, \tag{29}$$

$$[-\lambda\xi^2+(\lambda+2\mu+K)R^2+\lambda_0 a](-A\sinh Rd+B\cosh Rd)+[-\lambda\xi^2+(\lambda+2\mu+K)S^2+\lambda_0 b]\times(-C\sinh Sd+D\cosh Sd)-\mathrm{i}\xi P(2\mu+K)(E\cosh Pd-F\sinh Pd)-\mathrm{i}\xi Q(2\mu+K)\times(G\cosh Qd-H\sinh Qd)+\rho_L\omega^2F_2\sin Th=0, \tag{30}$$

$$\mathrm{i}\xi R(2\mu+K)[A\cosh Rd+B\sinh Rd]+\mathrm{i}\xi S(2\mu+K)[C\cosh Sd+D\sinh Sd]+[\mu\xi^2+(\mu+K)P^2-Kc'](E\sinh Pd+F\cosh Pd)+[\mu\xi^2+(\mu+K)Q^2-Kd']\times(G\sinh Qd+H\cosh Qd)=0, \tag{31}$$

$$\mathrm{i}\xi R(2\mu+K)[A\cosh Rd-B\sinh Rd]+\mathrm{i}\xi S(2\mu+K)[C\cosh Sd-D\sinh Sd]+[\mu\xi^2+(\mu+K)P^2-Kc'](-E\sinh Pd+F\cosh Pd)+[\mu\xi^2+(\mu+K)Q^2-Kd']\times(-G\sinh Qd+H\cosh Qd)=0, \tag{32}$$

$$Pc'(E\cosh Pd+F\sinh Pd)+Qd'(G\cosh Qd+H\sinh Qd)=0, \tag{33}$$

$$Pc'(E\cosh Pd-F\sinh Pd)+Qd'(G\cosh Qd-H\sinh Qd)=0, \tag{34}$$

$$R(A\cosh Rd+B\sinh Rd)+S(C\cosh Sd+D\sinh Sd)-\mathrm{i}\xi(E\sinh Pd+F\cosh Pd+G\sinh Qd+H\cosh Qd)-TF_1\cos Th=0, \tag{35}$$

$$R(A\cosh Rd-B\sinh Rd)+S(C\cosh Sd-D\sinh Sd)-\mathrm{i}\xi(-E\sinh Pd+F\cosh Pd-G\sinh Qd+H\cosh Qd)-TF_2\cos Th=0, \tag{36}$$

$$aR(A\cosh Rd+B\sinh Rd)+bS(C\cosh Sd+D\sinh Sd)=0, \tag{37}$$

$$aR(A\cosh Rd-B\sinh Rd)+bS(C\cosh Sd-D\sinh Sd)=0. \tag{38}$$

For non-trivial solution of these equations, the determinant of their coefficient matrix should vanish. For

$$T\neq 0 \quad \text{and} \quad Th\neq\frac{(2n-1)\pi}{2} \quad (n=1,2,\ldots),$$

this determinantal equation leads to the following frequency equations for symmetric (with index '+1') and antisymmetric (with index '−1') modes of vibrations, respectively

$$(aRM_2(\coth Sd)^{\pm1}-bSM_1(\coth Rd)^{\pm1})(Pc'N_2(\coth Pd)^{\pm1}-Qd'N_1(\coth Qd)^{\pm1})-(b-a)(d'-c')\xi^2M_3^2RSPQ(\coth Qd\coth Pd)^{\pm1}=-RS(b-a)\frac{\rho_L\omega^2}{T}\tan Th[\xi^2M_3(Qd'(\coth Qd)^{\pm1}-c'P(\coth Pd)^{\pm1})-(Qd'N_1(\coth Qd)^{\pm1}-c'PN_2(\coth Pd)^{\pm1})], \tag{39}$$

where

$$M_1=-\lambda\xi^2+(\lambda+2\mu+K)R^2+\lambda_0 a,\quad M_2=-\lambda\xi^2+(\lambda+2\mu+K)S^2+\lambda_0 b,$$

$$M_3=(2\mu+K),\quad N_1=\mu\xi^2+(\mu+K)P^2-Kc',\quad N_2=\mu\xi^2+(\mu+K)Q^2-Kd'.$$

It can be seen that equations in Eq. (39) exhibit implicit functional relationship between phase velocity and wavenumber, therefore, the symmetric and antisymmetric modes of Rayleigh–Lamb waves are dispersive in nature. Moreover, the tanh and coth functions are multiple valued functions, therefore there exist infinite number of modes of propagation.

Similarly, using the boundary conditions given in Set-II, we obtain the following frequency equations for symmetric (with index '+1') and antisymmetric (with index '−1') modes of propagation of Rayleigh–Lamb waves, respectively.

$$\begin{aligned}&(aM_2 - bM_1)[aN_2(\coth Sd)^{\pm 1} - bN_1(\coth Rd)^{\pm 1}][M_3 d'(\tanh Pd)^{\pm 1} - M_4 c'(\tanh Qd)^{\pm 1}]\\ &\quad = \frac{\rho_L}{T}\omega^2 \tan Th[(aS(\coth Sd)^{\pm 1} - bR(\coth Rd)^{\pm 1})\\ &\qquad \times (N_3 d' - N_4 c') - \mathrm{i}\xi(aN_2(\coth Sd)^{\pm 1} - bN_1(\coth Rd)^{\pm 1})(c' - d')].\end{aligned} \tag{40}$$

## 4. Limiting cases

### 4.1. Symmetric vibrations

(i) For waves long compared with the thickness of the plate, the quantity $\xi d$ is small and therefore $Rd$, $Sd$, $Pd$, and $Qd$ may be assumed small as long as $c$ is finite. In this case, $\tanh x \to x$ and from Eq. (39), we obtain the following frequency equation for symmetric modes of vibration:

$$\begin{aligned}&(aR^2M_2 - bS^2M_1)(N_2c' - N_1d') - R^2S^2\xi^2M_3^2(b-a)(d'-c')\\ &\quad = R^2S^2(b-a)\frac{\rho_L\omega^2}{T}\tan Th[\xi^2M_3(d'-c') - (N_1d' - N_2c')].\end{aligned} \tag{41}$$

In the absence of liquid layers, i.e. when $\rho_L = 0$, the above Eq. (41) reduces to

$$(aR^2M_2 - bS^2M_1)(N_2c' - N_1d') - R^2S^2\xi^2M_3^2(b-a)(d'-c') = 0. \tag{42}$$

This is the frequency equation for symmetric modes of vibration in a microstretch elastic plate with free boundaries in the present case. Further, if we neglect the microstretch property from the plate, then we shall be left with the problem of Lamb wave propagation in a micropolar elastic plate with free boundaries. Thus, by putting $\lambda_0 = \alpha_0 = \lambda_1 = 0$ and $b/a = 0$, Eq. (42) reduces to

$$[(2\mu + K)\xi^2 - \rho\omega^2][N_2c' - N_1d'] = \xi^2 S'^2(2\mu + K)^2(c' - d'), \tag{43}$$

where

$$S' = \sqrt{\xi^2 - \frac{\rho\omega^2}{\lambda + 2\mu + K}}.$$

This equation matches with the frequency equation as obtained by Nowacki and Nowacki [21] for the relevant problem apart from notations.

Again, in the absence of micropolarity, i.e. when $K = d'/c' = 0$, we obtain from Eq. (43) after some simplification

$$c^2 = 4\beta^2\left(1 - \frac{\beta^2}{\alpha^2}\right), \tag{44}$$

where $\alpha^2 = (\lambda + 2\mu)/\rho$ and $\beta^2 = \mu/\rho$. This equation exactly match with Lamb [1].

(ii) For very short waves as compared with the thickness of the plate, the quantity $\xi d$ is large, therefore, the quantities $Rd$, $Sd$, $Pd$ and $Qd$ are large as long as $c$ is finite. In this case, $\tanh x \to 1$ and Eq. (39) for

symmetric mode reduces to:

$$(aRM_2 - bSM_1)(Pc'N_2 - Qd'N_1) - RSPQ\xi^2 M_3^2(b-a)(d'-c')$$
$$= -RS(b-a)\frac{\rho_L\omega^2}{T}\tan Th[\xi^2 M_3^2(d'Q - Pc') - (d'QN_1 - Pc'N_2)]. \quad (45)$$

This is the frequency equation for Rayleigh waves in microstretch elastic half-space with liquid layers.

If we neglect the liquid layers, then the problem reduces to Rayleigh waves in microstretch elastic half-space. To obtain the Rayleigh wave dispersion equation in microstretch elastic half-space, we shall put $\rho_L = 0$ into Eq. (45) and obtaining

$$(aRM_2 - bSM_1)(Pc'N_2 - Qd'N_1) = RSPQ\xi^2 M_3^2(b-a)(d'-c'). \quad (46)$$

Again, if we remove the microstretch effect then the problem reduces to Rayleigh waves in micropolar elastic half-space. By putting $\lambda_0 = \alpha_0 = \lambda_1 = b/a = 0$ into Eq. (46), we obtain

$$M_2(Pc'N_2 - Qd'N_1) = -SPQ\xi^2 M_3^2(d'-c'). \quad (47)$$

This equation is the Rayleigh wave dispersion equation in a micropolar elastic half-space earlier obtained by De and Sengupta [22].

If we again neglect the micropolar effect, we shall obtain the Rayleigh wave dispersion equation in a uniform elastic half-space. Thus, putting $K = d'/c' = 0$ into Eq. (47), we obtain

$$\left(2 - \frac{c^2}{\beta^2}\right)^2 = 4\left(1 - \frac{c^2}{\alpha^2}\right)^{1/2}\left(1 - \frac{c^2}{\beta^2}\right)^{1/2}, \quad (48)$$

which is a well-known classical Rayleigh wave frequency equation in an elastic half-space.

### 4.2. Antisymmetric vibrations

(i) For waves long compared with the thickness of the plate, the quantity $\xi d$ is small, therefore, the quantities $Rd, Sd, Pd$ and $Qd$ are small. Using $\tanh x \simeq x - (x^3/3)$ into Eq. (39) for antisymmetric mode, we obtain the following equation:

$$(aM_2Y_1 - bM_1Y_2)(P^2c'N_2Z_1 - Q^2d'N_1Z_2) - P^2Q^2\xi^2M_3^2(b-a)(d'-c')Z_1Z_2$$
$$= -(b-a)\frac{\rho_L\omega^2}{Td}\tan Th[\xi^2 M_3(Q^2d'Z_2 - P^2c'Z_1) - (Q^2d'N_1Z_2 - P^2c'N_2Z_1)], \quad (49)$$

where

$$Y_1 = 1 - (Sd)^2/3, \quad Y_2 = 1 - (Rd)^2/3, \quad Z_1 = 1 - (Pd)^2/3, \quad Z_2 = 1 - (Qd)^2/3.$$

If we neglect the liquid layers, then by putting $\rho_L = 0$ into the above equation, we obtain

$$(aM_2Y_1 - bM_1Y_2)(P^2c'N_2Z_1 - Q^2d'N_1Z_2) = P^2Q^2\xi^2M_3^2(b-a)(d'-c')Z_1Z_2. \quad (50)$$

Now, if we further remove the microstretch effect from the plate, then Eq. (50) reduces to the following equation, after putting $\lambda_0 = \alpha_0 = \lambda_1 = 0$ and $b/a = 0$:

$$M_2\left(1 - \frac{(Sd)^2}{3}\right)\left(\frac{c'N_2}{Q^2Z_2} - \frac{d'N_1}{P^2Z_1}\right) = \xi^2 M_3^2(c'-d'), \quad (51)$$

where $M_2 = -\lambda\xi^2 + (\lambda + 2\mu + K)S^2$ and other symbols have their usual meanings. This equation is same as obtained by Nowacki and Nowacki [21] for the relevant problem.

If we further remove the micropolar effect from the plate, then by using $K = 0$ and $d'/c' = 0$, in Eq. (51), we obtain

$$c^2 = \frac{4}{3}(\xi d)^2\beta^2\left(1 - \frac{\beta^2}{\alpha^2}\right). \quad (52)$$

This equation coincides with the equation for classical elasticity as given in Ewing et al. [6] for relevant problem.

(ii) For very short waves compared with the thickness of the plate, the frequency equation (39) for antisymmetric modes of vibration can be reduced to Eq. (45), in a similar way as done in case of symmetric vibrations.

## 5. Special cases

(i) If we remove the liquid layers from both sides of the plate, then we shall be left with the problem of wave propagation in a microstretch plate with free faces. To do this, we shall put $\rho_L = 0$ into Eq. (39). The reduced frequency equations for symmetric (with index '+1') and antisymmetric (with index '−1') modes of vibrations for the said case are given by

$$[aRM_2(\coth Sd)^{\pm 1} - bSM_1(\coth Rd)^{\pm 1}][Pc'N_2(\coth Pd)^{\pm 1} - Qd'N_1(\coth Qd)^{\pm 1}] - (b-a)(d'-c')\xi^2 M_3^2 RSPQ(\coth Qd \coth Pd)^{\pm 1} = 0. \quad (53)$$

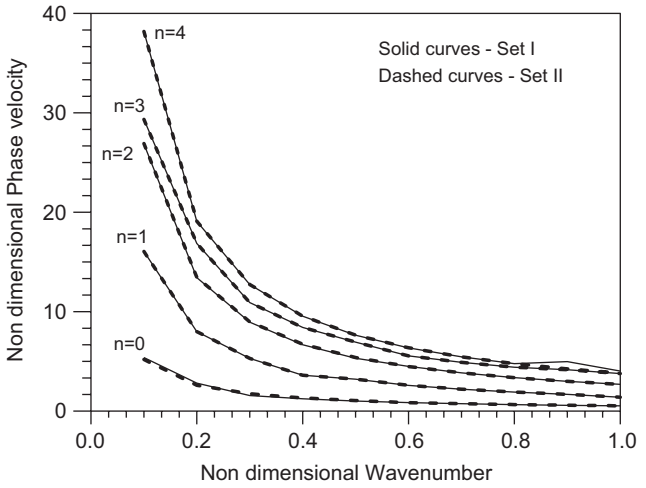


Fig. 2. Comparison of symmetric modes of microstretch plate bordered with liquid layers for Set-I and Set-II.

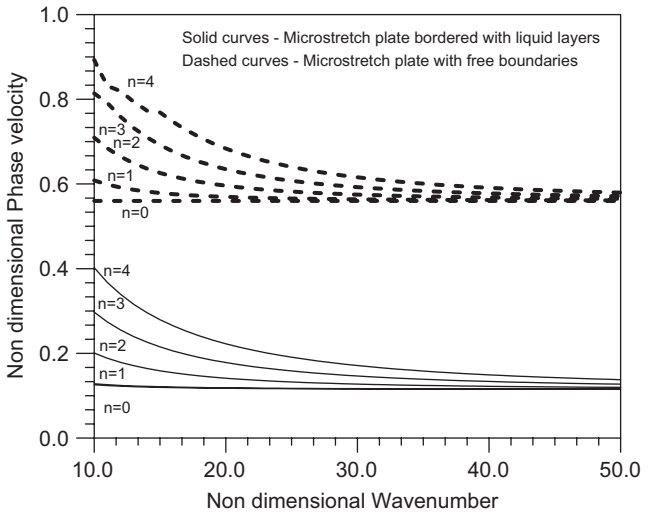


Fig. 3. Comparison of real parts of symmetric modes of microstretch plate bordered with liquid layers and with free boundaries.

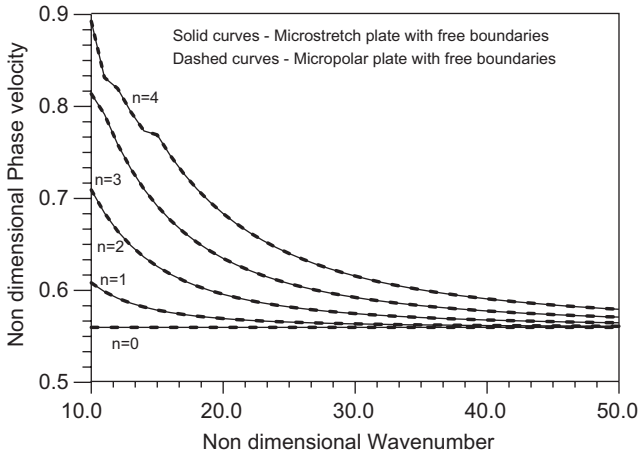


Fig. 4. Comparison of real parts of symmetric modes of microstretch plate and micropolar plate with free boundaries.

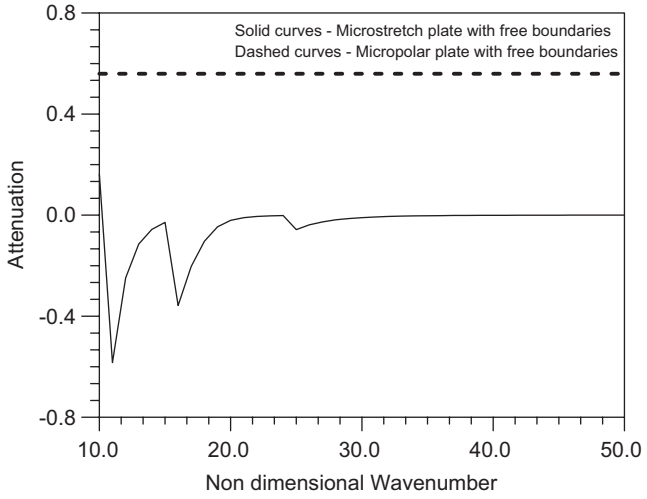


Fig. 5. Comparison of attenuation in symmetric fundamental mode of microstretch plate and micropolar plate with free boundaries.

(ii) When microstretch effect is neglected from the plate, we shall be left with the problem of Lamb wave propagation in micropolar plate bordered with liquid layers. In this case, we substitute $\lambda_0 = \lambda_1 = \alpha_0 = 0$ and $b/a = 0$ in Eq. (39) and obtaining equations for symmetric (with index '+1') and antisymmetric (with index '−1') mode, respectively, as

$$\begin{aligned}
&(\coth Sd)^{\pm 1}[-\lambda\xi^2 + (\lambda + 2\mu + K)S^2][(\mu\xi^2 + (\mu + K)P^2 - Kc')d'Q(\coth Qd)^{\pm 1} \\
&\quad - (\mu\xi^2 + (\mu + K)Q^2 - Kd')c'P(\coth Pd)^{\pm 1}] - \xi^2 PQS(2\mu + K)^2(d' - c')(\coth Qd \coth Pd)^{\pm 1} \\
&\quad = \rho_L\omega^2 \tan Th\left(\frac{S}{T}\right)[(\mu\xi^2 + (\mu + K)P^2 - Kc')Qd'(\coth Qd)^{\pm 1} - c'P[\mu\xi^2 + (\mu + K)Q^2 - Kd'] \\
&\quad \times (\coth Pd)^{\pm 1} - \xi^2(2\mu + K)[Pc'(\coth Pd)^{\pm 1} - Qd'(\coth Qd)^{\pm 1}]].
\end{aligned} \tag{54}$$

These equations exactly match with Eqs. (30) and (31) of Tomar [19] apart from notations.

Further, if we neglect the liquid layers, we shall be left with the problem of wave propagation in a micropolar plate with free boundaries. For this, putting $\rho_L = 0$ into Eq. (54), we obtain

$$(\coth Sd)^{\pm 1}[-\lambda\xi^2 + (\lambda + 2\mu + K)S^2][(\mu\xi^2 + (\mu + K)P^2 - Kc')d'Q(\coth Qd)^{\pm 1} - (\mu\xi^2 + (\mu + K)Q^2 - Kd')c'P(\coth Pd)^{\pm 1}] - \xi^2 PQS(2\mu + K)^2(d' - c')(\coth Qd \coth Pd)^{\pm 1} = 0, \quad (55)$$

which are the frequency equations for symmetric (with index '+1') and antisymmetric (with index '−1') modes for Lamb waves in micropolar elastic plate with free boundaries.

(iii) When $h \to \infty$, then $\tan Th \to$ i and the equations in Eq. (39) for symmetric (with index '+1') and antisymmetric (with index '−1') mode, respectively, reduce to the followings:

$$[aRM_2(\coth Sd)^{\pm 1} - bSM_1(\coth Rd)^{\pm 1}][Pc'N_2(\coth Pd)^{\pm 1} - Qd'N_1(\coth Qd)^{\pm 1}] - (b - a)(d' - c')\xi^2 M_3^2 RSPQ(\coth Qd \coth Pd)^{\pm 1}$$

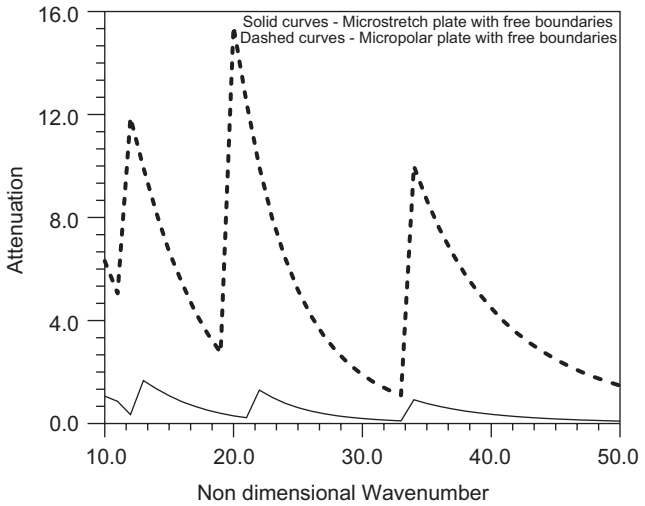


Fig. 6. Comparison of attenuation in symmetric first mode of microstretch plate and micropolar plate with free boundaries.

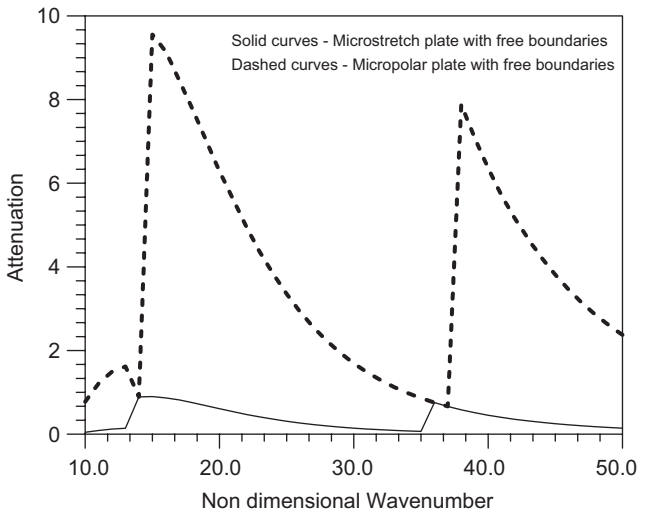


Fig. 7. Comparison of attenuation in symmetric second mode of microstretch plate and micropolar plate with free boundaries.

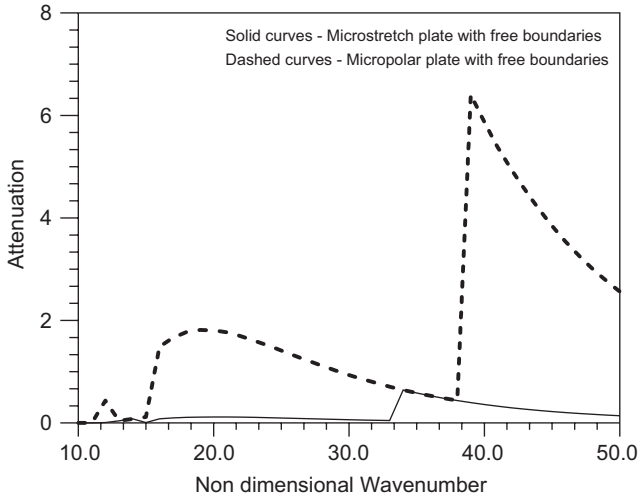


Fig. 8. Comparison of attenuation in symmetric third mode of microstretch plate and micropolar plate with free boundaries.

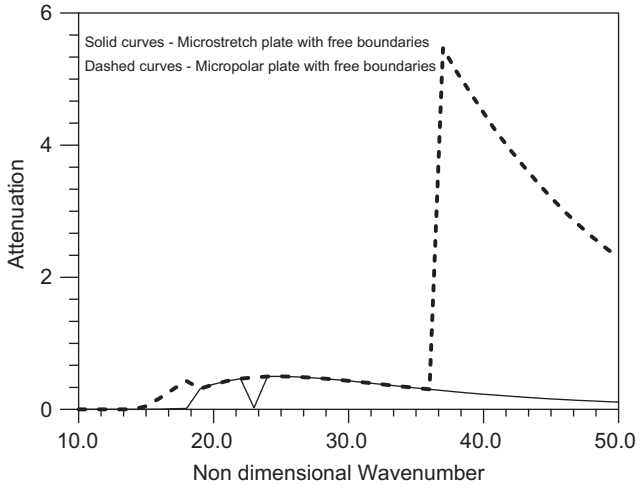


Fig. 9. Comparison of attenuation in symmetric fourth mode of microstretch plate and micropolar plate with free boundaries.

$$= -RS(b-a)\mathrm{i}\frac{\rho_L\omega^2}{T}[\xi^2 M_3[Qd'(\coth Qd)^{\pm 1} - c'P(\coth Pd)^{\pm 1}] - [Qd'N_1(\coth Qd)^{\pm 1} - c'PN_2(\coth Pd)^{\pm 1}]]. \quad (56)$$

These equations are, respectively, the dispersion equations for symmetric (with index '+1') and antisymmetric (with index '−1') modes of leaky Lamb waves in microstretch elastic plate bordered with identical inviscid liquid half-space on both sides.

(iv) When microstretch and micropolar effects are neglected from the plate, we shall make use of $K = \alpha_0 = \lambda_1 = \lambda_0 = 0$ and $b/a = 0$ and $d'/c' = 0$. Using these values into equations in Eq. (39), we obtain the equations for symmetric (with index '+1') and antisymmetric (with index '−1') modes of Lamb wave propagation in elastic plate bordered with liquid layers as

$$M_2N_2(\coth Sd \tanh Qd)^{\pm 1} - SQ\xi^2 M_3^2 = -S\frac{\rho_L\omega^2}{T}\tan Th(\tanh Qd)^{\pm 1}(\xi^2 M_3 - N_2). \quad (57)$$

Equations in Eq. (57) are the same as Eqs. (5) and (6) obtained for the relevant problem by Wu and Zu [2] apart from notations.

(v) If we neglect the liquid layers from the elastic plate in case (iv), we obtain the problem of Lamb wave propagation in elastic plate. Putting $\rho_L = 0$ in the case (iv), the equations reduce to

$$M_2 N_2 (\coth Sd \tanh Qd)^{\pm 1} - SQ\xi^2 M_3^2 = 0. \tag{58}$$

These equations can be re-written in the following well-known equations:

$$\left(2 - \frac{c^2}{c_2^2}\right)^2 \left(\frac{\tanh Qd}{\tanh Sd}\right)^{\pm 1} = 4\sqrt{\left(1 - \frac{c^2}{c_1^2}\right)\left(1 - \frac{c^2}{c_2^2}\right)}, \tag{59}$$

where $c_1^2 = (\lambda + 2\mu)/\rho$ and $c_2^2 = \mu/\rho$. These equations exactly match with those obtained by Lamb [1] for the relevant problem.

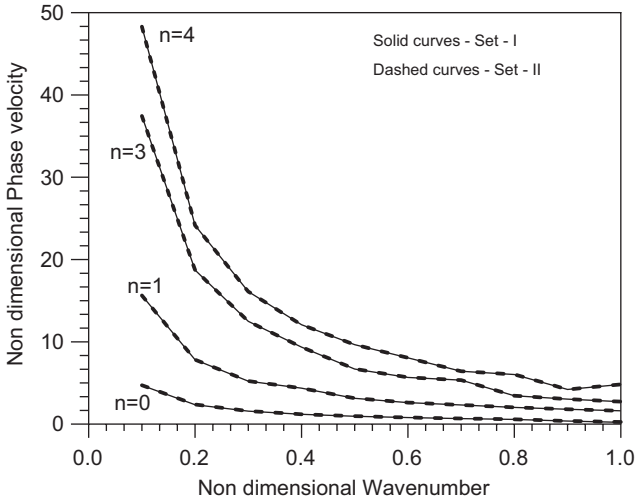


Fig. 10. Comparison of antisymmetric modes of microstretch plate bordered with liquid layers for Set-I and Set-II.

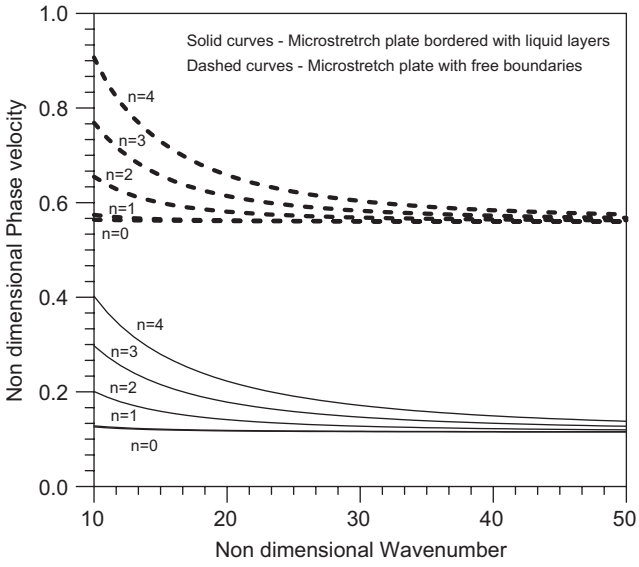


Fig. 11. Comparison of antisymmetric modes of microstretch plate bordered with liquid layers and with free boundaries.

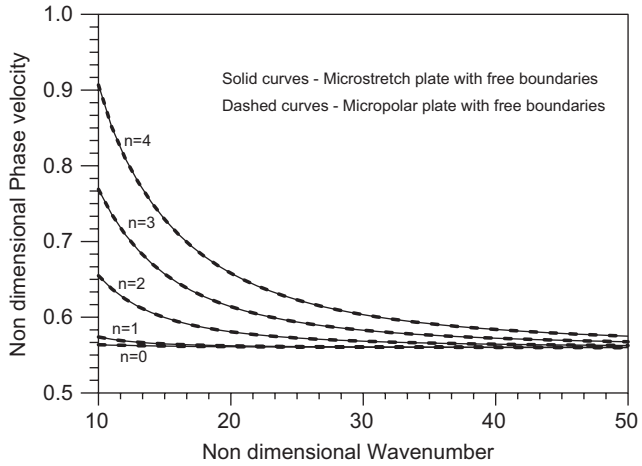


Fig. 12. Comparison of real parts of antisymmetric modes of microstretch plate and micropolar plate with free boundaries.

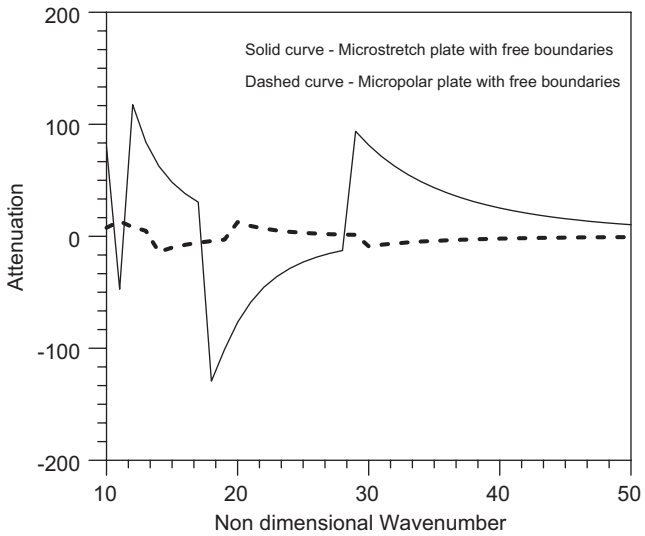


Fig. 13. Comparison of attenuation in antisymmetric fundamental mode of microstretch plate and micropolar plate with free boundaries.

It can be verified that if we neglect the micropolar effect, microstretch effect and liquid layers from the problem, then equations in Eq. (40) reduce to corresponding equations in Eq. (59) for Lamb waves in elastic plate given by Lamb [1].

## 6. Numerical results and discussions

Frequency equations for Rayleigh–Lamb waves are solved numerically for a particular model using functional iteration method. Following values of relevant elastic parameters have been taken.

For microstretch elastic plate, the values are

$$\lambda = 7.583 \times 10^{11}\,\mathrm{dyn/cm^2}, \quad \mu = 6.334 \times 10^{11}\,\mathrm{dyn/cm^2}, \quad K = 0.0149 \times 10^{11}\,\mathrm{dyn/cm^2},$$

$$\lambda_0 = 0.773 \times 10^{11}\,\mathrm{dyn/cm^2}, \quad \lambda_1 = 0.030 \times 10^{11}\,\mathrm{dyn/cm^2}, \quad \alpha_0 = 0.085 \times 10^{11}\,\mathrm{dyn},$$

$$\gamma = 2.89 \times 10^{11}\,\text{dyn}, \quad j = 0.000625\,\text{cm}^2, \quad \rho = 1.2\,\text{g/cm}^3, \quad d = 1.5\,\text{cm}$$

and for liquid layers the values are

$$\rho_L = 1.1\,\text{g/cm}^3, \quad \lambda_L = 0.245 \times 10^{11}\,\text{dyn/cm}^2, \quad h = 0.5\,\text{cm}.$$

We have computed the non-dimensional phase velocity $(c/V)$, $(V^2 = c_1^2 + c_3^2)$ at different values of non-dimensional wavenumber $(\xi d)$. The values of velocity ratio $(c/V)$ are computed from the frequency equation (39) obtained by using the boundary conditions given in Set-I and Eq. (40) obtained by using the boundary conditions given by Set-II for different values of wavenumber '$\xi d$'. For real values of $(\xi d)$, the real values of phase velocity $(c/V)$ are found for microstretch plate bordered with liquid layers and for micropolar plate bordered with liquid layers. The results obtained for symmetric modes (s-mode) and antisymmetric modes (a-mode) are depicted graphically through Figs. 2–18. In case of microstretch plate with free boundaries and in case of micropolar plate with free boundaries, the waves are found to attenuate.

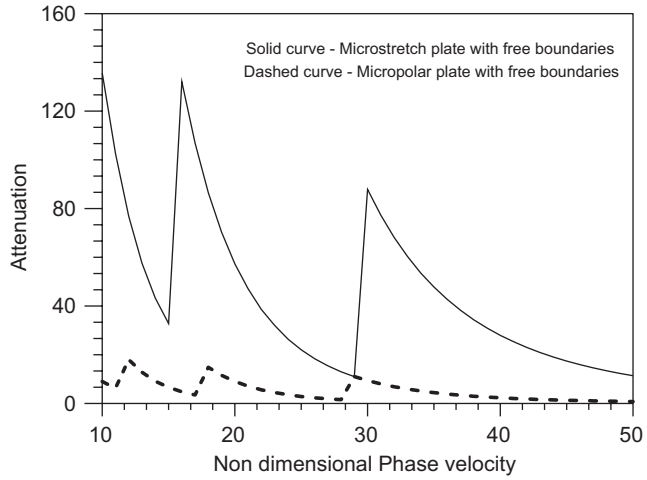


Fig. 14. Comparison of attenuation in antisymmetric first mode of microstretch plate and micropolar plate with free boundaries.

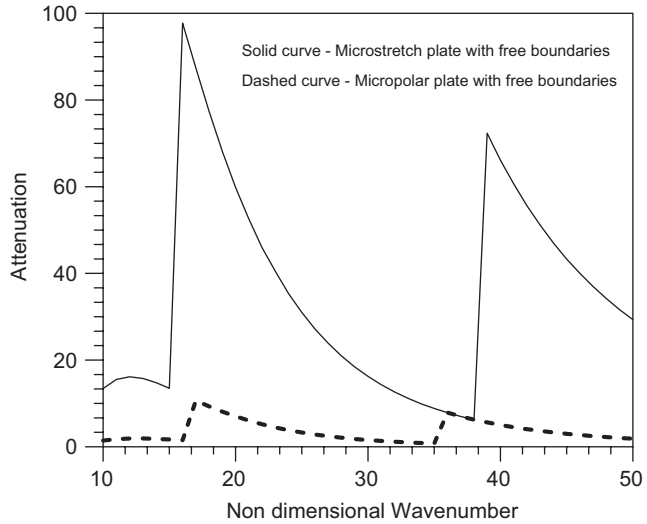


Fig. 15. Comparison of attenuation in antisymmetric second mode of microstretch plate and micropolar plate with free boundaries.

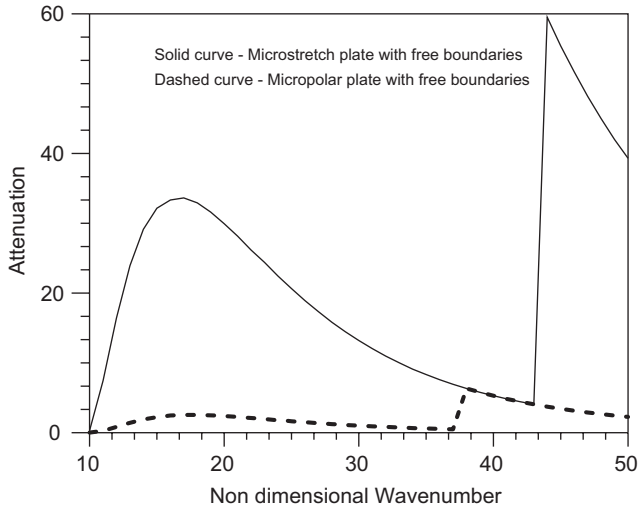


Fig. 16. Comparison of attenuation in antisymmetric third mode of microstretch plate and micropolar plate with free boundaries.

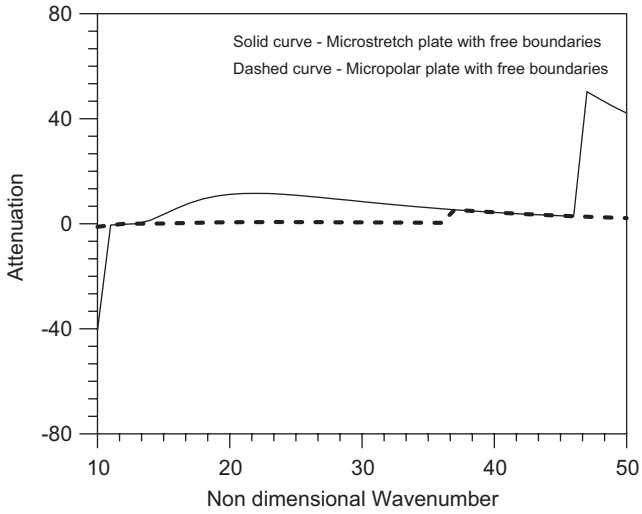


Fig. 17. Comparison of attenuation in antisymmetric fourth mode of microstretch plate and micropolar plate with free boundaries.

In Fig. 2, we have depicted the dispersion curves for fundamental, first, second, third and fourth symmetric modes of Rayleigh–Lamb wave propagation in microstretch plate bordered with liquid layers. It is clear from this figure that the dispersion curves for symmetric modes corresponding to the Set-I and Set-II of boundary conditions do not differ significantly. Thus, we conclude that one can choose any set of the boundary conditions.

In Fig. 3, we have depicted the dispersion curves for first five symmetric modes of vibration in microstretch plate bordered with liquid layers and in microstretch plate with free boundaries. It is found that for real values of wavenumbers, the phase velocity is real in microstretch plate bordered with liquid layers, while it is complex for microstretch plate with free boundaries. In this figure, the dotted curves correspond to the real part of the phase velocity. We note that the real part of phase velocity for microstretch plate with free boundaries is greater than that of the phase velocity of microstretch plate bordered with liquid layers. Thus, we conclude that the presence of the liquid layers results in decrease the phase velocity of the Rayleigh–Lamb waves in symmetric modes.

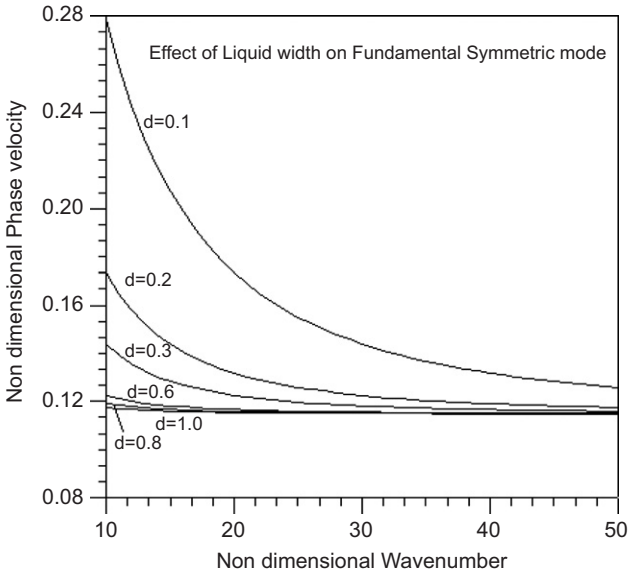


Fig. 18. Comparison of symmetric fundamental mode at different width of cladded liquid layers.

In Fig. 4, we have depicted the real parts of the phase velocities for the first five symmetric modes of vibration in microstretch plate with free boundaries and for micropolar plate with free boundaries. No significant difference between these velocities is observed. Thus, no considerable effect of microstretch property is noticed on the symmetric modes of Rayleigh–Lamb wave propagation.

Figs. 5–9 depict the comparison of attenuation coefficients for fundamental, first, second, third and fourth symmetric modes of microstretch plate and micropolar plate with free boundaries, respectively. The attenuation coefficients are found to be very small in magnitude, therefore to plot the variation of these coefficients, we have multiplied their original values by the factor $10^6$. Solid curve corresponds to the microstretch plate with free boundaries, while dotted curve corresponds to the micropolar plate with free boundaries. It is clear that there is a significant effect of microstretch property on the attenuation coefficient of the symmetric modes of Rayleigh–Lamb waves. We note that the presence of microstretch property is responsible for lowering down the attenuation of waves for symmetric modes.

Fig. 10 depicts the dispersion curves from fundamental to fourth antisymmetric modes of Rayleigh–Lamb wave propagation in a microstretch plate bordered with liquid layers corresponding to the boundary conditions given in Set-I and Set-II. The curves obtained are almost same for these two sets of boundary conditions. Thus, we again conclude that there is no significant difference in the phase velocity of antisymmetric modes of Rayleigh–Lamb waves for these two sets of boundary conditions.

Fig. 11 depicts the comparison of dispersion curves of fundamental to fourth modes of antisymmetric vibration in a microstretch plate bordered with liquid layers and in a microstretch plate with free boundaries. It is found that in the antisymmetric modes of propagation, the phase velocity in the microstretch plate with free boundaries is greater than that of in the microstretch plate bordered with liquid layers.

Fig. 12 depicts the dispersion curves for fundamental to fourth antisymmetric modes for microstretch plate and micropolar plate with free boundaries. We Note that there is no significant effect of microstretch property on real part of phase velocity for microstretch plate with free boundaries in antisymmetric modes.

Figs. 13–17 depict the attenuation coefficient for fundamental to fourth antisymmetric modes of Rayleigh–Lamb wave propagation of microstretch plate and of micropolar plate with free boundaries. Here solid curves and dotted curves correspond to microstretch plate and micropolar plate, respectively. Since the attenuation coefficients, in this case also, are found very small in magnitude, therefore, they have been plotted after multiplying their original values by a factor $10^6$. It is observed that attenuation is strongly affected by the presence of microstretch in antisymmmetric modes also and it increases the attenuation for all these five modes.

Fig. 18 depicts the dispersion curves for fundamental symmetric mode at different thickness of liquid layers. We see that as the width of liquid layers increases, the phase velocity for fundamental symmetric mode decreases.

## 7. Conclusions

In this paper, we have described the effect of microstretch property on the propagation of Rayleigh–Lamb waves in a microstretch plate cladded with inviscid liquid layers. We have two sets of boundary conditions at the interfaces of the plate and the liquid layers. Dispersion equations for symmetric and antisymmetric modes for microstretch plate cladded with inviscid and non-polar liquid layers are derived using both these sets of boundary conditions. The frequency equations are solved numerically and dispersion curves are depicted graphically. We conclude that

(i) The choice on the boundary conditions at the interfaces of the plate and the liquid layers is arbitrary. Results obtained from both the sets of boundary conditions give same dispersion curves for Rayleigh–Lamb wave propagation in symmetric and antisymmetric modes. So one can choose either Set-I or Set-II of the boundary conditions.
(ii) It is noted that the presence of cladded liquid layers in a microstretch plate decreases the phase velocity for both symmetric and antisymmetric modes of Rayleigh–Lamb wave propagation. For real values of wavenumbers, the frequency equations give real phase velocity, when plate is cladded with liquid layers, otherwise it gives complex values of phase velocity. Thus, the waves are non-attenuated, when plate is cladded with liquid layers, while the waves are found to be attenuated when both the faces of the plate are free.
(iii) There is no significant effect of microstretch property on the dispersion curves of real phase velocity of symmetric and antisymmetric modes in microstretch plate with free boundaries. This may be due to small values of microstretch parameters considered here. However, one can hope that for large values of microstretch parameters, the concerned dispersion curves might be affected significantly.
(iv) The attenuation is highly affected by the presence of microstretch in the plate with free boundaries for both the symmetric as well as the antisymmetric modes of Rayleigh–Lamb wave propagation.

## Acknowledgment

Dilbag Singh is thankful to Council of Scientific and Industrial Research, New Delhi for providing financial assistance in the form of Junior Research Fellowship.

## References

[1] H. Lamb, On waves in an elastic plate, *Proceedings of Royal Society, London, Series* 93 (1917) 114–128.
[2] J. Wu, Z. Zhu, The propagation of Lamb waves in a plate bordered with layers of a liquid, *Journal of Acoustical Society of America* 91 (1992) 861–867.
[3] Z. Zhu, J. Wu, The propagation of Lamb waves in a plate bordered with a viscous liquid, *Journal of Acoustical Society of America* 98 (1995) 1057–1064.
[4] J.N. Sharma, V. Pathania, S.K. Gupta, Thermoelastic Lamb waves in a transversely isotropic plate bordered with layers of inviscid liquid, *International Journal of Engineering Science* 41 (2003) 1219–1237.
[5] J.N. Sharma, V. Pathania, Thermoelastic waves in a plate bordered with layers of inviscid liquid, *Journal of Thermal Stresses* 26 (2003) 149–166.
[6] W. Ewing, W.S. Jardetzky, F. Press, *Elastic Waves in Layered Media*, McGraw-Hill, New York, 1957.
[7] I.A. Viktorov, *Rayleigh and Lamb Waves: Physical Theory and Applications*, Plenum Press, New York, 1967.
[8] K.F. Graff, *Wave Motion in Elastic Solids*, Dover, New York, 1991, pp. 431–463.
[9] D.E. Chimenti, Guided waves in plates and their use in materials characterization, *Applied Mechanics Review* 50 (1997) 247–284.
[10] A.L. Shuvalov, On the theory of wave propagation in anisotropic plates, *Proceedings of Royal Society London, Series A: Mathematical, Physical and Engineering Sciences* 456 (2000) 2197–2222.
[11] W.P. Rogers, Elastic property measurement using Rayleigh–Lamb waves, *Research in Non-Destructive Evaluation* 6 (1995) 185–208.
[12] A.C. Eringen, E.S. Suhubi, Nonlinear theory of simple micro-elastic solids—I, *International Journal of Engineering Science* 2 (1964) 189–203.

[13] E.S. Suhubi, A.C. Eringen, Nonlinear theory of micro-elastic solids—II, *International Journal of Engineering Science* 2 (1964) 389–404.
[14] A.C. Eringen, Linear theory of micropolar elasticity, *Journal of Mathematics and Mechanics* 15 (1966) 909–923.
[15] A.C. Eringen, Theory of micropolar elasticity, in: H. Liebowitz (Ed.), *Fracture*, Vol. II, Academic Press, New York, 1968 (Chapter 7).
[16] A.C. Eringen, Mechanics of micromorphic materials, in: H. Gortler (Ed.), *Proceedings of Eleventh Congress of Applied Mechanics*, Springer, New York, 1964.
[17] A.C. Eringen, Theory of thermo-microstretch elastic solids, *International Journal of Engineering Science* 28 (12) (1990) 1291–1301.
[18] A.C. Eringen, *Microcontinuum Field Theories—I: Foundations and Solids*, Springer, New York, 1999.
[19] S.K. Tomar, Wave propagation in a micropolar elastic layer, *Proceedings of National Academy of Sciences, India* 72(A) IV (2002) 339–350.
[20] S.K. Tomar, Wave propagation in a micropolar elastic plate with voids, *Journal of Vibration and Control* 11 (2005) 849–863.
[21] W. Nowacki, W.K. Nowacki, Propagation of monochromatic waves in an infinite micropolar elastic plate, *Bulletin de l'Academie Polonaise des Sciences, Serie des Sciences Techniques* 17 (1969) 45–53.
[22] S.N. De, P.R. Sengupta, Surface waves in micropolar elastic medium, *Bulletin de l' Academie Polonaise des Sciences, Serie des Sciences Techniques* 22 (1974) 213–222.